

ELECTRONIC PROPERTIES OF CONDUCTING SYSTEMS

Mixed 1D-2D quantum electron transport in percolating gold film

E. Yu. Belyayev, B. I. Belevtsev,^{a)} and Yu. A. Kolesnichenko

*B. Verkin Institute of Low Temperature Physics and Engineering, National Academy of Sciences of Ukraine,
47 Lenin Ave, Kharkov 61103, Ukraine*

(Submitted September 3, 2010)

Fiz. Nizk. Temp. **37**, 409–417 (April 2011)

A gold film (mean thickness ≈ 3.5 nm) was deposited in high vacuum on a single-crystal sapphire substrate at a temperature of 70 K. The transport properties of the film at low temperature reveal simultaneous 1D and 2D quantum interference effects of weak localization and electron-electron interaction. This behavior is found to be determined by inhomogeneous electron transport at the threshold of a thickness-controlled metal-insulator transition. © 2011 American Institute of Physics. [doi: 10.1063/1.3592529]

I. INTRODUCTION

Metal-insulator transitions (MIT) in disordered systems are still a basic challenge in solid-state physics. One of the principal causes of MIT is increased lattice disorder (so called Anderson transitions). It has been found theoretically that a two-dimensional (2D) system of noninteracting electrons should be insulating at any degree of disorder on approaching zero temperature.¹ Electron-electron interactions, however, play a crucial role in 2D transport, especially at low temperatures,^{2–4} so that MIT in 2D systems is theoretically possible and has been confirmed experimentally.^{2,3} Two types of crystal-lattice disorder that affect electron motion in conducting solids are usually considered. The first is associated with perturbations of the scattering potentials on an atomic scale: impurities, vacancies, and so on, and is often called microscopic. At the same time, MIT can also take place in inhomogeneous systems such as disordered mixtures of a metal and an insulator, granular metals, and the like,^{5,6} where the scale of disorder is well above interatomic distances, and where moving electrons must overcome insulating regions (or boundaries) between metallic clusters (grains). This second type of disorder is called macroscopic. MIT in systems with macroscopic disorder is inevitably associated with (classical or quantum) percolation effects in electron transport.

Many experimental studies of MIT have been made on ultrathin metal films with step-by-step increases in the film thickness.^{3,5} The nominal thickness increments are usually in the range 0.05–0.1 Å, or much less than interatomic distances. This raises the following questions: do the films remain homogeneous in thickness with these small increments, and are the films homogeneous at all during an MIT, which occurs at some critical thickness, d_c ? It is known from studies of this type of MIT, that d_c is in the range 1–5 nm, depending on the film structure (crystalline or amorphous) and the substrate material. The smallest values of d_c (1–1.5 nm) have been found in quench-condensed amorphous Bi and Ga films with thin underlayers of amorphous Ge.⁷ In most cases, the sheet resistance of films, R_{\square} , with thicknesses $d \approx d_c$ is on the order of 10 k Ω , which is comparable with the quantum of resistance, $R_Q = R_{\square} = a\hbar/e^2$, where $\hbar/e^2 \approx 4.1$ k Ω and a is on the order of unity. R_Q is often

regarded as a characteristic resistance for 2D MIT. It is evident that condensed films with $R_{\square} \geq R_Q$ are discontinuous, so that percolating effects should be important.

Here we study the transport properties of quench-condensed gold films with thicknesses of about 3.56 nm and R_{\square} about 5 k Ω above 10 K. These films have a weakly nonmetallic temperature dependence of the resistance, with logarithmic behavior above 10 K and a somewhat stronger dependence at low temperatures. The films are characterized by quantum interference effects in electron transport. Above 3 K only 2D transport effects were found, whereas, below 3 K both one-dimensional (1D) and 2D transport effects can be distinguished. This reflects the inhomogeneous structure (and corresponding electron transport) of the film near thickness-controlled MITs in ultrathin metallic films.

II. EXPERIMENTAL TECHNIQUE

Gold film was prepared by thermal evaporation from a Mo boat onto a substrate of polished single-crystal sapphire. The size of the film regions was 2×0.1 mm. The substrate was initially etched in hot aqua regia, then washed in distilled water and etched in boiling bichromate, then again washed in distilled water, and finally dried in a desiccator.

Deposition of the film on a prepared substrate and subsequent *in situ* measurement of its transport properties were carried out in a high-vacuum cryostat containing ³He and a superconducting solenoid. Oil-free vacuum pumps were used to reach a pressure of about 10^{-7} Pa. A system of sliding screens (masks) was used for deposition of gold contacts (at room temperature) and subsequent deposition of the gold film (at $T \approx 70$ K at a rate of 0.05 nm/s). The initial purity of the deposited gold was 99.99%. The residual gas pressure during deposition was about 5×10^{-6} Pa. The resistance of the film was monitored during its growth (with an applied voltage $U_{\text{appl}} = 1$ V), and deposition was interrupted when R_{\square} reached about 4.4 k Ω . According to our previous studies,⁸ the structure of gold films with R_{\square} around 5 k Ω deposited under similar conditions is close to the percolation threshold. The nominal film thickness, determined by a quartz sensor, is 3.56 nm. The prepared sample was held at the preparation temperature (70 K) for 12 h, until the small variations in its resistance owing to structural relaxation

typical of films deposited on cold substrates came to an end. The magnetoresistive measurements were carried out *in situ* at lower temperatures of 0.4–30 K in magnetic fields from -0.05 to $+5$ T. The resistance was determined by measuring the current for a preset applied voltage U_{appl} . Most of the measurements were made with $U_{\text{appl}} = 0.2, 1, \text{ and } 5$ V, although other voltages were also used, especially when determining the current-voltage characteristic at different temperatures (see below).

III. RESULTS AND DISCUSSION

A. General characterization of the transport properties of the film

The conducting state of these films was found to correspond to that at the threshold of thickness-controlled MIT. The temperature dependence of the resistance has nonmetallic ($dR/dT < 0$) character, which above 10 K and at high enough applied voltage is logarithmic ($\Delta R \propto \ln T$) (Fig. 1). At low temperatures (below 5 K), the resistance has an obvious dependence on the applied voltage (Figs. 1 and 2). It can be seen (Fig. 2) that at $T = 5$ K a decrease in voltage leads to only a slight increase in resistance so that at this temperature (and above it) Ohm's law is obeyed to a good approximation. At lower temperatures, however, an exponential increase in resistance with decreasing voltage can be seen at low voltages ($U_{\text{appl}} < 50$ mV) (inset to Fig. 2), although for $U_{\text{appl}} \geq 2$ V the non-ohmic behavior is slight. It should be noted that the same voltage dependence [$R \propto \exp(1/U_{\text{appl}})$] at low temperatures (but with far larger amplitude in R variations) has been observed in Ref. 8 in percolating gold film obtained under the same conditions as in this study. But with a smaller nominal thickness (3.25 nm), the film in Ref. 8 was accordingly more resistive and demonstrated a full transition from strong to weak electron localization with increasing U_{appl} , whereas, in the film studied here only some indications of this type of behavior are found.

The transport properties, therefore, confirm the inhomogeneous structure of the film. This is certainly related to its spatially nonuniform thickness. The small effective thick-

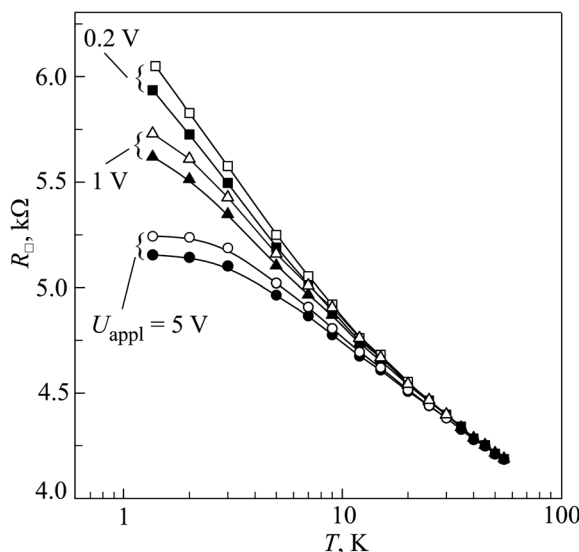


FIG. 1. Temperature dependence of the sheet resistance of a gold film for different applied dc voltages (U_{appl}). The $R_{\square}(T)$ curves are shown for zero magnetic field (solid symbols) and for $H = 4.2$ T (hollow symbols).

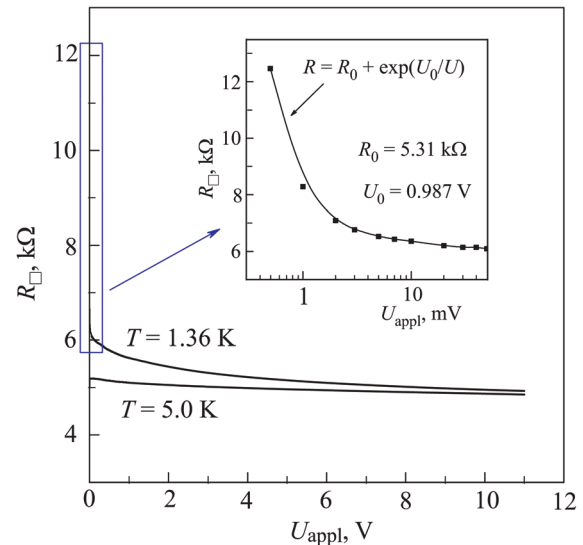


FIG. 2. Resistance as a function of applied voltage U_{appl} at low temperatures. The inset shows R_{\square} vs U_{appl} in the region of low voltages for $T = 1.36$ K.

ness of the film (3.56 nm), high values of R_{\square} (about 6 kΩ and higher) and the rather strongly pronounced non-ohmic behavior of its conductivity at low temperatures indicate that the film is partially discontinuous. This means that it consists of metallic islands (or percolating clusters) separated by tunnel barriers. Two types of barriers are possible: (a) vacuum gaps between adjacent islands on an insulating substrate, and (b) narrow and thin constrictions (bridges) between islands in the case of weak contacts between neighboring islands. In any case, this sort of system can be regarded as similar to a two-dimensional granular metal. These suggestions are fully in line with the results of studies of quench-condensed (substrate temperature between 4 K and 77 K) Au films.⁹ It has been found⁹ that the critical nominal thickness, d_{cr} , marking the onset of conductivity is about 2 nm for quench-condensed Au films and this agrees reasonably well with our results. It follows from Ref. 9 that quench-condensed Au films deposited on a weak-binding substrate (as in this study) form a 2D disordered array of weakly-connected islands at thicknesses moderately greater than d_{cr} . The grain diameter, d_G , in this type of Au film is in the range $10 \text{ nm} < d_G < 20 \text{ nm}$ (Ref. 9).

A quasi-granular 2D structure of the film is also supported by the following: it is known that the product ρl [where $\rho (=R_{\square}d)$ and l are the resistivity and mean-free path, respectively] is a characteristic constant for typical metals. For gold, $\rho l \approx 8.43 \times 10^{-16} \text{ } \Omega\text{m}^2$ in the quasi-free electron approximation. Using this formula, we obtain $l \approx 0.05$ nm for the film studied here. Such a low nominal value (less than the interatomic distance) clearly indicates an inhomogeneous structure for our film that is on the threshold of thickness-controlled MIT. The high resistivity is determined by low intergrain tunnel conductivity; however, intragrain conductivity can be far higher. We shall take the distinctive morphology of quench-condensed ultrathin gold films into account in our analysis.

B. Quantum interference effects in the film conductivity

The logarithmic dependence ($\Delta R \propto \ln T$) found for the thin film studied here (Fig. 1) implies that it is related to

quantum weak localization (WL) and electron-electron interaction (EEI) effects in the conductivity of 2D systems.⁴ The two-dimensional conditions for the occurrence of these effects are: $d < L_\phi$, L_T , where d is the film thickness, $L_\phi = (D\tau_\phi)^{1/2}$ is the diffusion length for phase relaxation, $L_T = (\hbar D/kT)^{1/2}$ is the thermal coherence length in the normal metal, D is the electron diffusion coefficient, and τ_ϕ is phase relaxation time. The lengths L_ϕ and L_T are attributed to WL and EEI effects, respectively. Macroscopic disorder (percolating and/or granular structures) can have a dramatic influence on the WL and EEI effects,¹⁰ including complete suppression for strong enough disorder. At the same time, a rather weak macroscopic disorder has no significant influence on these quantum effects. In particular, the system behaves as homogeneous with respect to WL and EEI effects if the relevant lengths [$L_\phi(T)$ and L_T] are larger than the characteristic inhomogeneity scale (for example, the percolation correlation length ξ_p or grain diameter d_G in a 2D granular metal).

For a homogeneous 2D system the contribution of WL and EEI to the temperature variation in the conductivity in zero magnetic field is given by⁴

$$\Delta\sigma(T) = \frac{e^2}{2\pi^2\hbar} \left\{ -\left[\frac{3}{2} \ln \frac{\tau_\phi^*}{\tau} - \frac{1}{2} \ln \frac{\tau_\phi}{\tau} \right] + \lambda_T^D \ln \frac{kT\tau}{\hbar} \right\} \quad (1)$$

where τ is the elastic electron relaxation time, $\tau_{\text{in}}^{-1} = \tau_{\text{in}}^{-1} + 2\tau_s^{-1}$; $(\tau_\phi^*)^{-1} = \tau_{\text{in}}^{-1} + (4/3)\tau_{so}^{-1} + (2/3)\tau_s^{-1}$; τ_{in} is the phase relaxation time owing to inelastic scattering, and τ_{so} and τ_s are spin relaxation times for the electrons owing to spin-orbit and spin-spin scattering, respectively. λ_T^D is the interaction constant in the diffusive channel, which is close to unity for typical metals. The time τ_{in} is temperature dependent, i.e., $\tau_{\text{in}}^{-1} \propto T^p$, where the exponent p depends on the mechanism for inelastic scattering. The first term in Eq. (1) corresponds to WL effects and the second, to EEI.

Equation (1) contains the well known logarithmic correction to the conductivity, which can be rewritten as⁴

$$\frac{\Delta R}{R} = -a_T \frac{e^2 R_\square^{\text{eff}}}{2\pi^2\hbar} \ln \left(\frac{kT\tau}{\hbar} \right), \quad (2)$$

where a_T is on the order of unity, with its exact value determined by the dominant mechanisms for phase relaxation in a specific system.

It is known that gold is characterized by a strong spin-orbit interaction [$\tau_{so} \ll \tau_{\text{in}}(T)$], which determines the specific value of a_T , and causes the appearance of positive magnetoresistance owing to the WL effect,⁴ as is usually observed in gold films,^{8,11} including the film studied here (see Fig. 1 and the more detailed information below). For strong spin-orbit scattering and neglecting the spin-spin interaction [$\tau_{so} \ll \tau_{\text{in}}(T)$ and $\tau_s \gg \tau_{so}, \tau_{\text{in}}$], Eq. (1) gives $a_T = 1 - p/2$, where the 1 comes from the EEI effect and second part is determined by the WL effect, with p being the exponent in temperature dependence $\tau_{\text{in}}^{-1} \propto T^p$ for the dominant mechanism of phase relaxation.

Generally, phase relaxation is determined by two main factors: electron-electron and electron-phonon interactions, so that $\tau_{\text{in}}^{-1} = \tau_{ee}^{-1} + \tau_{ep}^{-1}$, where τ_{ee} and τ_{ep} are the corresponding times. It has been found for electron-phonon inter-

action processes in disordered (R_\square up to $\approx 500 \Omega$) gold films that $\tau_{ep}^{-1} \propto T^p$ with the exponent p ranging between 2 and 2.8.¹¹ According to Ref. 11, electron-phonon scattering predominates in the phase relaxation of gold films only above 10 K. Below this temperature it is found that $\tau_{\text{in}}^{-1} \propto T$, attributable to electron-electron scattering. It is known that the rate of phase relaxation owing to electron-electron scattering in 2D systems is determined by collisions with small energy transfer ($\Delta E \ll kT$) (Ref. 4)

$$\tau_{ee}^{-1}(T) = \frac{\pi kT}{\hbar} \frac{e^2 R_\square}{2\pi^2\hbar} \ln \left(\frac{\pi\hbar}{e^2 R_\square} \right). \quad (3)$$

Increasing disorder leads to dominant EEI in the phase relaxation (that is $\tau_{ee}^{-1} \gg \tau_{ep}^{-1}$). Since our films are far more disordered than those of Ref. 11, the temperature range for dominant EEI should be much wider. In this case, can assume that $p = 1$, so that $a_T = 1/2$ is to be expected.

We now consider the experimental values of a_T . It is found in our films, $a_T \approx 1.15$ for $U_{\text{appl}} = 0.2$ V at $T > 8$ K and is close to unity for higher voltages above 5 K (Figs. 1 and 3). When using Eq. (2) to determine a_T we have taken the measured macroscopic resistance R_\square^{exp} as R_\square^{eff} . This can be done only for homogeneous systems. If a system is assumed to be inhomogeneous, then R_\square^{eff} should be a fitting parameter.¹² We have examined this question. For instance, on analyzing the logarithmic $R(T)$ dependence at $U_{\text{appl}} = 5$ V we found $R_\square^{\text{eff}} = 5.28$ k Ω for $a_T = 1$. This value of the sheet resistance lies within range of variation of R_\square with temperature at $U_{\text{appl}} = 5$ V (Fig. 1), so that at this voltage the system behaves as a homogeneous system above 5 K.

The derived values of $a_T \approx 1$ do not agree with the $a_T \approx 1/2$ expected for systems with strong spin-orbit interactions. So it seems that only EEI contributes to the logarithmic $R(T)$ dependence. It seems likely that the WL correction is significantly suppressed in our films for some reason, so that EEI contribution predominates in $R(T)$, so that $a_T \approx 1$. The

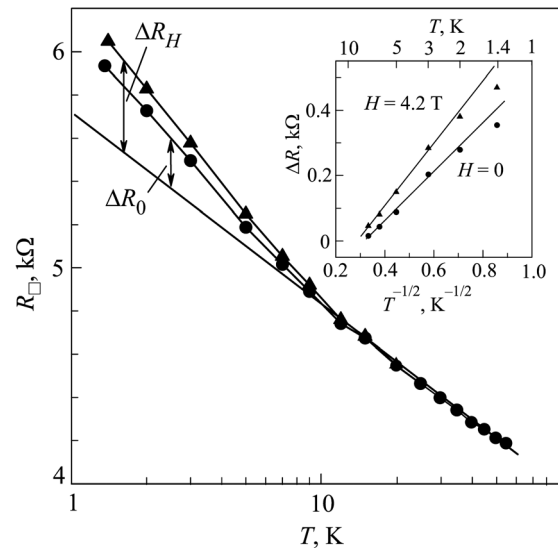


FIG. 3. The sheet resistance of the gold film as a function of temperature measured at $U_{\text{appl}} = 0.2$ V at zero magnetic field (\bullet) and $H = 4.2$ T (\blacktriangle). The $R(T)$ curves have a logarithmic dependence above $T \approx 8$ K. Below that temperature, deviations ΔR from a logarithmic dependence of the resistance develop with decreasing temperature. The temperature behavior of these low-temperature deviations is plotted as ΔR vs $T^{-1/2}$ in the inset.

total suppression of WL is possible in some cases, for example, by applying a sufficiently strong magnetic field ($H > H_\phi = \hbar c / 4eL_\phi^2$) (Ref. 4). Figure 1 shows that an applied field $H = 4.2$ T, far higher than H_ϕ (as will be clear below), only has a weak effect on the slope of the linear part of ΔR as a function of $\ln T$ above $T \approx 8$ K, so that it appears that WL is significantly suppressed in the film even in zero field. This situation is possible in inhomogeneous (percolating or granular) 2D films.⁶ In a system consisting of rather large grains separated by weak tunnel barriers, the existence of a WL correction (as in homogeneous systems) is determined by closed electron trajectories with self-intersections that increase the probability of back-scattering.⁴ The size of these trajectories is approximately L_ϕ . The EEI correction is determined by length L_T . Generally, in a quasi-particle description of electrons, the relation $L_T \ll L_\phi$ holds.⁴ In any case, for the WL and EEI corrections to show up clearly in the $R(T)$ dependences, both lengths L_ϕ and L_T should exceed the characteristic inhomogeneity scale of the system (for example, grain size d_G). Since $L_\phi \gg LT$, the electron trajectories which determine the WL effect should overlap more grains (and more intersections with grain boundaries) than those connected with the EEI effect, so that weak intergrain connections can suppress WL effects more strongly than EEI effects.

Figure 1 shows that $R(T)$ has a logarithmic dependence only for sufficiently high temperatures. $R(T)$ begins to deviate from $\ln T$ behavior below 5 K for $U_{\text{appl}} = 5$ V, and seems to go to saturation at sufficiently low temperatures. In this case, an overheating effect cannot be excluded. The overheating should be, however, be less with decreasing voltage. In fact, saturation ceases at $U_{\text{appl}} = 1$ V, and at the lower voltage $U_{\text{appl}} = 0.2$ V an increased rate of rise of $R(T)$ with decreasing temperature is actually observed at low temperatures (Fig. 1). This last case is illustrated more clearly in Fig. 3. Below 9 K a deviation from a $\ln T$ -dependence develops; it is shown in the inset as $\Delta R = f(T^{-1/2})$. This will be discussed in detail below.

The magnetoresistance (MR) data also reflect the inhomogeneous structure of the film. Figure 4 gives a general

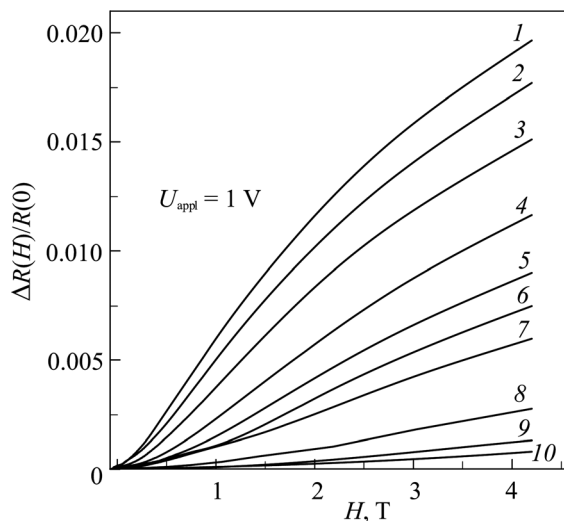


FIG. 4. Magnetoresistance curves of the film measured for an applied voltage $U_{\text{appl}} = 1$ V with the magnetic field normal to the film at T , K: 1.4 (1), 2 (2), 3 (3), 5 (4), 7 (5), 9 (6), 12 (7), 15 (8), 20 (9), 25 (10).

view of MR curves and their variations with temperature. Except at low fields ($H \leq 0.02$ T) and low temperatures ($T \leq 3.1$ K) (see below), the magnetoresistive curves agree with to the standard expression for MR owing to the WL effect in 2D systems:⁴

$$\Delta\sigma(H) = \frac{e^2}{2\pi^2\hbar} \left\{ \frac{3}{2}f_2\left(\frac{4eDH\tau_\phi^*}{\hbar c}\right) - \frac{1}{2}f_2\left(\frac{4eDH\tau_\phi}{\hbar c}\right) \right\} \quad (4)$$

where $f_2(x) = \ln(x) + \Psi(1/2 + 1/x)$, and Ψ is the digamma function. $f_2(x) \approx x^2/24$ for $x \ll 1$, and $f_2(x) \propto \ln x$ for $x \gg 1$. For the films studied here, the contribution of EEI to MR is negligible, so we omit the corresponding formulas.

The observed positive MR (Fig. 4) is expected for gold films with strong spin-orbit scattering. For this case [$\tau_{so} \ll \tau_{\text{in}}(T)$], Eq. (4) can be rewritten as⁴

$$\frac{\Delta R(H)}{R} = R_{\square}^{MR} \frac{e^2}{4\pi^2\hbar} f_2\left(\frac{4eHL_\phi^2}{\hbar c}\right). \quad (5)$$

We have found that Eq. (5) describes the experimental $R(H)$ dependences for $H \leq 1$ T adequately with small deviations at higher fields. Equation (4) describes the experimental $R(H)$ well over the entire range of fields, and the two equations have been used to derive the $L_\phi(T)$ dependence.

For homogeneous systems, the measured macroscopic resistance R_{\square}^{exp} can be substituted for R_{\square}^{MR} when analyzing the experimental data using Eqs. 4 or 5. R_{\square}^{MR} is the resistance on the scale of L_ϕ , and in an inhomogeneous sample can be less than the macroscopic resistance measured on much larger scale. In this case, R_{\square}^{MR} should be a fitting parameter.^{12,13} We have found that the computed values of R_{\square}^{MR} are actually somewhat lower than R_{\square}^{exp} (by about 20%). This difference is not, however, crucial and we have not found that it affects the calculated values of L_ϕ significantly.

The temperature dependence of $L_\phi(T)$ in the range 1.4–30 K is shown in Fig. 5. $L_\phi(T)$ is essentially independent on the applied voltage. In particular, in the range 3–10 K, the

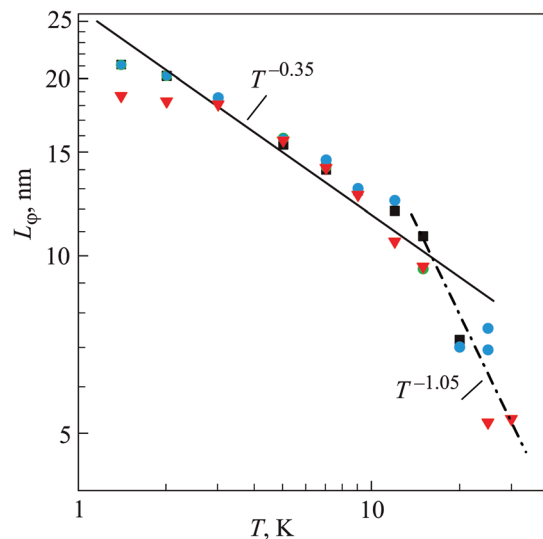


FIG. 5. Calculated temperature dependence of the phase relaxation length $L_\phi(T)$ in a film according to Eq. 4 for different magnitudes of U_{appl} , V: 0.2 (■), 1.0 (●), 5.0 (▼).

data for different U_{appl} practically coincide. Above $T \approx 10$ K the data become noisier owing to the smaller magnitude of MR in this range. At low temperatures (below 3 K), the effect of U_{appl} on L_ϕ is evident. In this range the $L_\phi(T)$ values tend to saturate with decreasing temperature below 3 K. The following temperature dependences $L_\phi(T)$ were found: $L_\phi(T) \propto T^{-0.35}$ (3 – 15 K) and $L_\phi(T) \propto T^{-1.05}$ (15 – 30 K). Since $L_\phi \propto T^{-p/2}$, the first case corresponds to $p \approx 0.7$ and the second to $p \approx 2.1$. We discuss these features of $L_\phi(T)$ in the next section.

C. Enhanced percolation character of electron transport at low temperatures and 1D effects on the film conductivity

At low temperatures we found a weak but quite distinct anomaly in the MR behavior in the low-field range. It is shown on a large scale in Fig. 6. This anomaly vanishes with increasing field and is suppressed with rising temperature up to $T \approx 3.1$ K (Fig. 7). The field at which the MR anomaly reaches saturation (and a transition to 2D MR behavior) increases with decreasing temperature and lies within the range 0.01–0.03 T (Fig. 7). At low fields ($H \leq 0.004$ T) the MR in the range of this anomaly has a quadratic dependence, $\Delta R(H)/R(0) \propto H^2$ (Fig. 8). The temperature dependence of the maximum MR at the anomaly (at the saturation field) is shown in the inset to Fig. 8.

It should be noted that we have seen this type of anomaly more than once at sufficiently low temperatures in other fairly disordered gold films (close to the thickness controlled percolation threshold). This allows us to assert that this low-temperature MR anomaly, and the above-mentioned deviations of $R(T)$ from logarithmic behavior at low temperatures (Fig. 3), are indications of 1D effects in film conductivity caused by an inhomogeneous (granular) film structure near the percolation threshold. Indications of mixed 1D-2D conductivity in percolating gold films were first reported in Ref. 10. Other 1D interference effects had been studied in specially made narrow films.^{12,14–16} The theory of quantum interference (WL and EEI) effects in 1D conductors has been developed in Refs. 4, 17, and 18.

Before further analysis and discussion of 1D effects in the film we have studied, the principal causes of appearance of these effects in ultrathin films should be considered. As

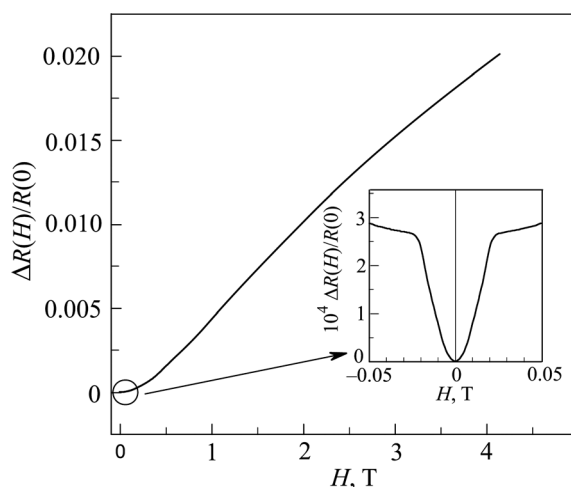


FIG. 6. Magnetoresistance curve at $T = 1.38$ K and $U_{\text{appl}} = 0.2$ V. The inset is an enlarged view of low-field part of the curve.

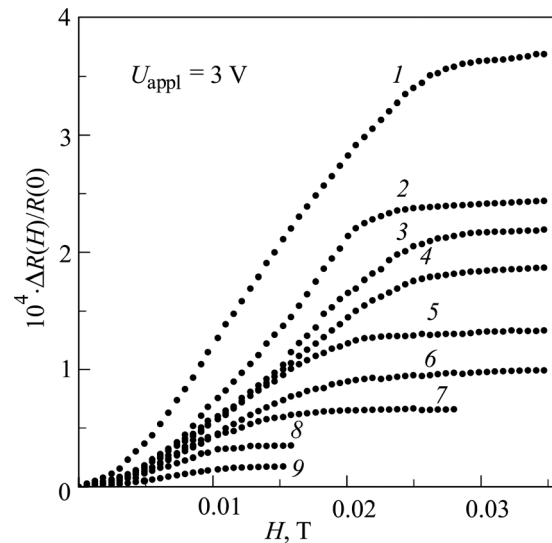


FIG. 7. Temperature evolution of the low-field anomaly in the MR attributed to 1D effects in the transport properties at T , K: 0.38 (1), 1.38 (2), 1.58 (3), 1.7 (4), 2.0 (5), 2.3 (6), 2.5 (7), 3 (8), 3.1 (9).

noted above, a film near the thickness-controlled percolation threshold consists of weakly connected islands (grains). The intergrain connections are determined by narrow constrictions, which can make tunnel junctions (like point contacts). In real quasi-island films near the percolation threshold, the intergrain constrictions (contacts) are not the same throughout the system, so that the conductivity is percolating. It is determined by the presence of optimal chains of grains with maximum probability of tunnelling for adjacent pairs of grains forming the chain. At low enough temperatures, tunnelling can be activated. In conditions of activated conductivity, the number of conducting chains decreases with decreasing temperature, so that at low enough temperatures a percolation network can consist of just a few conducting channels or even a single conducting path.¹⁹ This appears to be a general trend for disordered systems, and especially for 2D systems. For example, it has been shown theoretically,²⁰ that increasing in disorder in 2D systems leads to formation

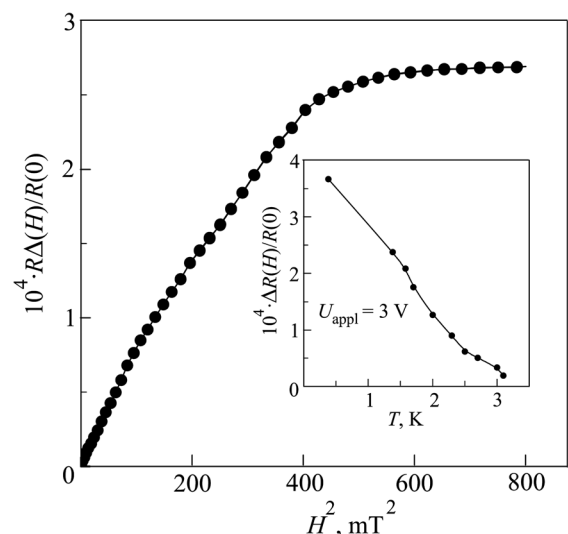


FIG. 8. MR as a function of the square of the magnetic field at $T = 1.38$ K, $U_{\text{appl}} = 0.2$ V. The inset shows the temperature variation of the saturation MR at the low-field MR anomaly.

of a narrow channel along which electrons can propagate throughout a disordered sample.

This suggests that a sufficiently thin percolating film can manifest mixed (1D and 2D) behavior with regard to interference effects in its conductivity. In this case, as in Ref. 10, it appears that the quantum correction to the conductivity has two contributions,

$$\frac{\Delta R(T, H)}{R} = \left(\frac{\Delta R(T, H)}{R} \right)_{1D} + \left(\frac{\Delta R(T, H)}{R} \right)_{2D}, \quad (6)$$

where the subscripts 1D and 2D indicate the corresponding contributions. The relative contributions of the two terms are temperature and magnetic-field dependent, so that, for example, the 1D term can even disappear at sufficiently high T or H .

Expressions for the 2D corrections were given above. For further discussion some valid 1D expressions are needed. The conditions for the appearance of 1D interference effects in electron transport are that both characteristic lengths, $L_T = (\hbar d/kT)^{1/2}$ and $L_\varphi = (D\tau_\varphi)^{1/2}$, must be greater than the width W , and thickness, d , of the 1D wire. It is known^{4,14,16} that 1D effects become apparent only at low temperatures where the main contribution to the phase breaking is from electron-electron scattering with small energy transfer.^{4,17,18} This, the so-called Nyquist phase-breaking mechanism, is especially important for low-dimensional systems.^{4,16,18} For 2D systems the Nyquist time is given by Eq. (3). For 1D systems this time is denoted by τ_N , and corresponding phase relaxation rate is given by^{4,18}

$$\tau_N^{-1} = \left[\left(\frac{e^2 R_\square}{\hbar} \right) \left(\frac{kT}{\hbar} \right) \left(\frac{\sqrt{2D}}{W} \right) \right]^{2/3} \propto T^{2/3}. \quad (7)$$

The characteristic phase-relaxation length for this process is $L_N = (D\tau_N)^{1/2} \propto T^{-1/3}$.

In line with our suggestion about mixed (1D and 2D) behavior of the film conductivity at low temperatures, we have compared the deviations of $R(T)$ from logarithmic 2D behavior at low temperatures (Fig. 3) with the available 1D equations. EEI correction to the resistance of a single film strip (for $W < L_T$) is⁴

$$\frac{\Delta R_{\text{int}}(T)}{R} = \frac{e^2 R_\square}{2\hbar W} L_T \propto T^{-1/2}, \quad (8)$$

where R_\square^{str} is the sheet resistance of the strip. This quantum correction increases with decreasing temperature as $T^{-1/2}$, in fairly good agreement with the $\Delta R(T)$ curve shown in the inset to Fig. 3. It should be noted that the $\Delta R \propto T^{-1/2}$ dependence for this film also occurs at high magnetic fields which completely suppress the WL effect, so that this behavior should be attributed solely to the EEI effect. Similar behavior corresponding to Eq. (8) has been previously seen in 1D Au films.^{12,15}

Of course, the WL effect can also affect quantum 1D transport.^{4,18} However, since gold is characterized by strong spin-orbit scattering (antilocalization), the corresponding correction, $\Delta R_{\text{loc}}(T)$, is negative and R should decrease with decreasing temperature. It has been found in 1D gold films that at sufficiently low temperatures, the EEI effect predomi-

nates in the quantum correction.^{12,16} Apparently this occurs in the gold film studied here, as well.

We now consider in more detail the low-field anomaly of MR at low temperatures (Figs. 6 and 7), which we have also attributed to 1D effects. MR of 1D systems in low magnetic fields is determined exclusively by WL.⁴ At sufficiently low temperatures, phase relaxation is determined by Nyquist mechanism so that $\tau_N \ll \tau_{\varphi 0}(H=0)$, where $\tau_{\varphi 0}$ is phase relaxation time owing to all other phase-breaking mechanisms. In the case of strong spin-orbit scattering, the WL correction to the resistance of a 1D film for magnetic fields perpendicular to the film plane is^{4,16,17}

$$\frac{\Delta R_{\text{loc}}(T, H)}{R_0} = -0.31 \frac{e^2 R_\square^{\text{str}}}{\hbar W} [1/L_N^2 + 1/D\tau_H]^{-1/2}, \quad (9)$$

where $\tau_H = 12L_H^4/DW^2$ and $L_H = \sqrt{\hbar c/2eH}$. Equation (9) shows that at low fields ($L_N^2 \ll D\tau_H$), the increase in the resistance in field H is

$$\begin{aligned} \frac{\Delta R_{\text{loc}}(T, H) - \Delta R_{\text{loc}}(T, 0)}{R_0} &\approx \frac{0.31 e^2 R_\square^{\text{str}} L_N^3}{2 \hbar W D\tau_H} \\ &= \frac{0.31 e^2 R_\square^{\text{str}} L_N^3 W}{2 \hbar 12L_H^4} \propto H^2/T. \end{aligned} \quad (10)$$

The quadratic dependence of the MR on magnetic field for low fields shows up clearly (Fig. 8). The temperature dependence of the MR is difficult to determine exactly because of the narrow temperature range of the anomaly. We have found, however, that this dependence is strong (inset to Fig. 8) and for 1.4–3 K it varies (but rather approximately) as $1/T$, as can be expected. It should also be mentioned that the amplitude of MR attributed to 1D WL found in this study ($\Delta R(H)/R$ of the order of 10^{-4}) agrees well with that found for other 1D metal films, including Au films.^{16,21–23}

Making a quantitative comparison with Eq. (10) and obtaining values of L_N from it appears to be quite difficult (or even, at first glance, practically impossible), since we do not actually have exact values for two of the parameters: the sheet resistance R_\square^{str} of the 1D strip and its width W . The macroscopic resistance $R_\square^{\text{exp}} \approx 5.2 \text{ k}\Omega$ of the film can be substituted for R_\square^{str} , but this can produce some error in the calculated values of L_N since it is expected that $R_\square^{\text{str}} \ll R_\square^{\text{exp}}$. A rough estimate of W can be made, given that in 1D films the transition from the 1D to 2D WL behavior for the MR takes place when L_H becomes smaller than the width W with increasing field.¹⁶ It follows from Fig. 7 that in the film studied here, the transition field H_{tr} , at which the MR anomaly saturates, depends on temperature. The magnitude of H_{tr} rises from $\approx 0.013 \text{ T}$ to $\approx 0.03 \text{ T}$ with decreasing temperature from $T = 3 \text{ K}$ to $T = 0.38 \text{ K}$, which implies a drop in W from $\approx 160 \text{ nm}$ to $\approx 100 \text{ nm}$ for this temperature variation (if we take the magnetic lengths L_H for these values of H_{tr} as the values of W). A decrease in W with decreasing temperature is not surprising and, furthermore, is quite expected in light of the reasons and conditions discussed above for the formation of 1D percolation structures in quench-condensed ultra-thin films.

Taking the above nominal values of W and $R_\square^{\text{exp}} \approx 5.2 \text{ k}\Omega$, we calculated L_N at different temperatures using

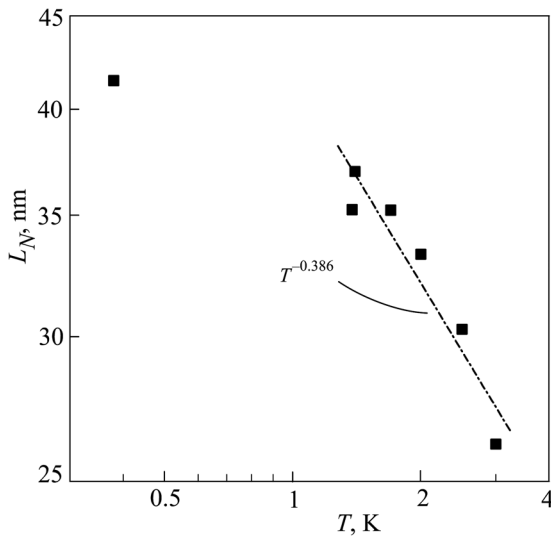


FIG. 9. Temperature dependence of the Nyquist length L_N calculated using Eq. (10) for $U_{\text{appl}} = 3$ V.

Eq. (10) for low-field MR. The result is shown in Fig. 9, which shows that in the range 1.5–3 K the calculated values of L_N are proportional to $T^{-0.386}$ which is fairly close to the theoretical prediction $L_N = (D\tau_N)^{1/2} \propto T^{-1/3}$. These values of L_N appear to be rather larger than the lengths $L_\phi = (D\tau_\phi)^{1/2}$ derived from the 2D MR curves in the same range 1.4–3 K (compare Figs. 5 and 9). It is important to mention as well that these values of L_N exceed the characteristic inhomogeneity scale of this granular film, i.e., the grain size, which, according to Ref. 9, is between 10 and 20 nm in quench-condensed ultrathin gold films. This is a necessary condition for observation of WL effects in granular or island films. Unfortunately, it is not possible to find the corresponding relaxation times, τ_N and τ_ϕ , since we cannot determine the electron diffusion coefficients D for the 1D and 2D cases in the inhomogeneous percolating film studied here.

It should be noted that calculated values of L_N are rather smaller than the estimated width W of the inferred 1D strip(s) in this film. As indicated above, this may be related to the uncertainty in the value of R_{\square}^{str} derived using Eq. (10): R_{\square}^{str} could be as much as ten times smaller than the value used here (5.2 k Ω). The uncertainty in R_{\square}^{str} should not, however, affect appreciably the temperature dependence $L_N(T)$ (Fig. 9).

For both the 1D and 2D WL interference effects in this film, the derived phase relaxation lengths seem to saturate on going to low temperatures (Figs. 5 and 9). The saturation is more pronounced for higher U_{appl} (Fig. 5); this may be because of an overheating effect. But the saturation persists even at lower U_{appl} , and this may be determined by the 2D inhomogeneous granular structure as suggested in Ref. 24.

Now we examine more closely the $L_\phi(T)$ curve derived from an analysis of MR in the 2D case using Eqs. (4) and (5). At 3–15 K, a $L_\phi \propto T^{-0.35}$ dependence was found (Fig. 5). At first glance this seems unexpected since at low temperatures in 2D systems the phase relaxation owing to EEI should dominate with a rate $\tau_{ee}^{-1} \propto T$ given by Eq. (3), and $L_\phi \propto T^{-1/2}$ as is usually observed in sufficiently homogeneous gold films.^{11,25} As indicated above, the diffusion length for phase relaxation has a general temperature de-

pendence $L_\phi \propto T^{-p/2}$, where p depends on mechanism of phase relaxation ($\tau_\phi \propto T^{-p}$). It is known that in percolating gold films the experimental values of p are often smaller than in homogeneous films. For example, in Refs. 12 and 25, respectively, $L_\phi \propto T^{-1/3}$ and $L_\phi \propto T^{-0.35}$ dependences were found, with fitting to Eq. (4) for the 2D WL, while $L_\phi \propto T^{-1/2}$ is expected for $p = 1$. In the first case,¹² this was attributed to the influence of 1D regions in the percolating gold film and, in the second,²⁵ anomalous electron diffusion for inhomogeneous films was invoked. In any case it is clear that this effect in the film studied here is determined by the inhomogeneity of the film.

The data obtained here show that with increasing temperature the film becomes more homogeneous with respect to quantum interference effects: 1D effects in MR disappear above 3 K (Figs. 7 and 8) and, $R(T)$ becomes purely logarithmic above 12 K, as expected for 2D systems (Fig. 3). $L_\phi(T)$ follows this tendency, changing to a $L_\phi(T) \propto T^{-1.05}$ dependence (Fig. 5) that corresponds to $p = 2.1$ above 15 K. This agrees with results for disordered, but sufficiently homogeneous, gold films,¹¹ where this has been convincingly attributed to the influence of electron-phonon phase relaxation.

In conclusion, we have found that the low-temperature transport properties of an inhomogeneous ultra-thin quench-condensed gold film reveal simultaneous quantum interference 1D and 2D weak localization and electron-electron interaction effects. With increasing temperature the film behaves as if it were more homogeneous and only 2D effects are seen. The observed behavior can be explained by inhomogeneous electron transport at the threshold of a thickness-controlled metal-insulator transition.

This work was supported in part by the program “Structure and Properties of Nanosystems” (Subsection 1.3.) of the National Academy of Sciences of Ukraine.

^{a)}Email: belevtsev@ilt.kharkov.ua

¹E. Abrahams, P. W. Anderson, D. C. Licciardello, and T. V. Ramakrishnan, *Phys. Rev. Lett.* **42**, 673 (1979).

²D. M. Basko, I. L. Aleiner, and B. L. Altshuler, *Ann. Phys.* **321**, 1126 (2006).

³V. F. Gantmakher and V. I. Dolgoplov, *Usp. Fiz. Nauk* **178**, 3 (2008); V. F. Gantmakher and V. I. Dolgoplov, *ibid.* **180**, 3 (2010).

⁴B. L. Altshuler and A. G. Aronov, *Electron-Electron Interactions in Disordered Systems*, edited by A. L. Efros and M. Pollak (North-Holland, Amsterdam, 1985), p. 1.

⁵B. I. Belevtsev, *Usp. Fiz. Nauk* **160**, 65 (1990) [*Sov. Phys. Usp.* **33**, 36 (1990)].

⁶I. S. Beloborodov, A. V. Lopatin, V. M. Vinokur, and K. B. Efetov, *Rev. Mod. Phys.* **79**, 469 (2007).

⁷H. M. Jaeger, D. B. Haviland, and A. M. Goldman, *Phys. Rev. B* **34**, 4920 (1986); N. Marković, C. Christiansen, and A. M. Goldman, *Phys. Rev. Lett.* **81**, 5217 (1998).

⁸B. I. Belevtsev, E. Yu. Belyaev, Yu. F. Komnik, and E. Yu. Kopeichenko, *Fiz. Nizk. Temp.* **23**, 965 (1997) [*Low Temp. Phys.* **23**, 724 (1997)].

⁹K. L. Ekinci and J. M. Valles, Jr., *Acta Mater.* **46**, 4549 (1998); *Phys. Rev. B* **58**, 4347 (1998).

¹⁰A. Palevskii and G. Deutscher, *Phys. Rev. B* **34**, 431 (1986).

¹¹B. I. Belevtsev, Yu. F. Komnik, and E. Yu. Beliayev, *Phys. Rev. B* **58**, 8079 (1998).

¹²M. E. Gershenson, P. M. Echternach, H. M. Bozler, A. L. Bogdanov, and B. Nilsson, *Phys. Rev. Lett.* **74**, 446 (1995).

¹³A. V. Butenko, E. I. Bukhshtab, and V. V. Pilipenko, *Fiz. Nizk. Temp.* **10**, 773 (1984) [*Sov. J. Low Temp. Phys.* **10**, 407 (1984)].

- ¹⁴S. Wind, M. J. Rooks, V. Chandrasekhar, and D. E. Prober, *Phys. Rev. Lett.* **57**, 633 (1986).
- ¹⁵W. D. Williams and N. Giordano, *Phys. Rev. B* **33**, 8146 (1986).
- ¹⁶P. M. Echternach, M. E. Gershenson, H. M. Bozler, A. L. Bogdanov, and B. Nilsson, *Phys. Rev. B* **48**, 11516 (1993); *ibid.* **50**, 5748 (1994).
- ¹⁷B. L. Altshuler and A. G. Aronov, *Pis'ma Zh. Eksp. Teor. Fiz.* **33**, 515 (1981) [*JETP Lett.* **33**, 499 (1981)].
- ¹⁸B. L. Altshuler, A. G. Aronov, and D. E. Khmel'nitskii, *J. Phys. C* **15**, 7367 (1982).
- ¹⁹P. Sheng, *Philos. Mag.* **B 65**, 357 (1992).
- ²⁰P. Markoř, *Physica B* **405**, 3029 (2010).
- ²¹J. J. Lin and N. Giordano, *Phys. Rev. B* **33**, 1519 (1986).
- ²²A. P. Heraud, S. P. Beaumont, C. D. W. Wilkinson, P. C. Main, J. R. Owers-Bradley, and L. Eaves, *J. Phys. C* **20**, L249 (1987).
- ²³F. Pierre, A. P. Gougam, A. Anthore, H. Pothier, D. Esteve, and Norman O. Birge, *Phys. Rev. B* **68**, 085413 (2003).
- ²⁴A. V. Germanenko, G. M. Minkov, and O. E. Rut, *Phys. Rev. B* **64**, 165404 (2001).
- ²⁵G. Dumpich and A. Carl, *Phys. Rev. B* **43**, 12074 (1991); A. Carl, G. Dumpich, Ch. Buchal, and B. Stritzker, *Z. Phys. B* **90**, 261 (1993).

This article was published in English in the original Russian journal. Reproduced here with stylistic changes by AIP.